Nuclear Magnetic Resonance and Diffuse-Reflectance Infrared Fourier Transform Spectroscopy of Biosolids-Derived Biocolloidal Organic Matter

ARTICLE *in* ENVIRONMENTAL SCIENCE AND TECHNOLOGY · JUNE 2003

Impact Factor: 5.33 · DOI: 10.1021/es020821z · Source: PubMed

4 AUTHORS, INCLUDING:

Jingdong Mao
Old Dominion University
126 PUBLICATIONS **2,558** CITATIONS
SEE PROFILE

Lakhwinder S. Hundal
Metropolitan Water Reclamation District of G…
46 PUBLICATIONS **1,051** CITATIONS
SEE PROFILE

Klaus Schmidt-Rohr
Brandeis University
255 PUBLICATIONS **8,997** CITATIONS
SEE PROFILE

Environ. Sci. Technol. **2003**, *37,* 1751−1757

Nuclear Magnetic Resonance and Diffuse-Reflectance Infrared Fourier Transform Spectroscopy of Biosolids-Derived Biocolloidal Organic Matter

J.-D. MAO,[†] L. S. HUNDAL,[‡] K. SCHMIDT-ROHR,*[,†] AND M. L. THOMPSON*[,§]

Department of Chemistry and Department of Agronomy, Iowa State University, Ames, Iowa 50011, and Research & Development Department, Metropolitan Water Reclamation District of Greater Chicago, 6001 West Pershing Road, Cicero, Illinois 60804

We extracted the acid-soluble portion of municipal biosolids, fractionated it by both molecular weight (MW) and hydrophobicity, and used various solid-state nuclear magnetic resonance (NMR) methods and diffuse-reflectance infrared Fourier transform (DRIFT) spectroscopy to characterize the fractions. Spectroscopic characterization of the MW components of the biosolids-derived organic matter fractions revealed the presence of functionally distinct groups of compounds. Quantitative ^{13}C NMR, CH spectral editing, and several two-dimensional NMR experiments show that the high-MW hydrophilic fraction in particular is structurally simple, consisting predominantly of N-acetylated polysaccharides, perhaps derived from bacterial peptidoglycans. In the high-MW hydrophobic fraction, aromatic compounds were present in addition to the N-acetylated polysaccharides. Infrared spectroscopy confirmed that hydrophilic fractions were dominated by carbohydrates and indicated that the lower-MW fractions lacked amide moieties. Complementary interpretations of the DRIFT and NMR spectra improved our knowledge of the components separated by this fractionation scheme, allowing better characterization of biosolids organic matter. Moreover, fractionation based on both MW and hydrophobicity may prove useful in detailed characterization of the structure of biosolids-derived organic matter and other similarly heterogeneous natural organic matter in soils and sediments.

Introduction

Primary wastewater solids that are processed to meet federal and state regulations for disposal are called *biosolids*. Disposal of biosolids by land application is increasingly more common in highly urbanized and industrialized countries. Heavy land application of biosolids may change the amount and composition of dissolved organic matter (DOM) in the soil (*1*, *2*). Although much of the potentially mobile fraction of DOM that is applied in biosolids undergoes microbial transformation, a portion of it may move through the soil to shallow aquifers, particularly through continuous channels and fractures. In many soils, DOM is likely to play an active role in transport of organic (pesticides and hydrocarbons) and inorganic (trace metals) pollutants as well as excess plant nutrients (*3*−*5*). Detailed chemical and physical characterization of biosolids-derived DOM is therefore helpful to predict its impact on the fate and transport of both pollutants and plant nutrients in soils.

Many reports have appeared in the literature regarding characterization of DOM in soil (e.g., ref *6*), in streamwater (e.g., ref *7*), and in biosolids-amended soils (e.g., refs *8* and *9*). Several previous investigations of humic and fulvic acids in biosolids have identified major functional groups by using infrared spectroscopy (e.g., refs *10*−*12*). In an early study of biosolids-derived fulvic acid with nuclear magnetic resonance (NMR) spectroscopy, Sposito et al. (*13*) identified both aromatic and aliphatic components. But characterization of biosolids-derived organic matter is difficult because of the physical and chemical heterogeneity of these materials. Fractionation based on both the physical and the chemical characteristics may prove helpful to separate more homogeneous components of biosolids. Leenheer (*14*) used XAD-8 resin chromatography to separate DOM into various components based on their relative hydrophobicity. Although other separation methods exist to fractionate DOM (electrophoresis, ion exchange, size exclusion chromatography, ultrafiltration, field-flow fractionation) (e.g., refs *15* and *16*), Leenheer's fractionation procedure has been widely adopted.

In this study, we fractionated the acid-soluble portion of biosolids-derived organic matter by both molecular weight (MW) and hydrophobicity. We characterized the fractions by several advanced solid-state NMR methods and diffuse-reflectance infrared Fourier transform (DRIFT) spectroscopy. Our objectives were to identify the functional groups and structures in DOM fractions, testing the hypothesis that the fractionation procedure resulted in chemically distinct classes of organic components.

Experimental Section

Samples and Fractionation of Biosolids-Derived Organic Matter. Samples of anaerobically digested biosolids were collected at the Ames Water Pollution Control Facility (Ames, IA). An outline of our fractionation procedure is given in Figure 1, and further details are presented in the Supporting Information for this paper and elsewhere (*2*, *17*). The acid-soluble fraction we isolated corresponds to the operational definition of fulvic acid, yet the degree to which it had been "humified" during anaerobic digestion is uncertain. To maintain objectivity in nomenclature, we use the term *biosolids-derived organic matter* (BOM) to refer to the acid-soluble organic material recovered from the biosolids. In addition, we adopt the adjective *biocolloidal* for the BOM with an apparent MW > 3.5 kDa, following Leenheer et al. (*18*).

The BOM was concentrated to 50 mg of C/L using vacuum-rotary evaporation at 40 °C and then separated into hydrophilic and hydrophobic components by passing it through XAD-8 resin columns. Effluent from the columns was defined as the total hydrophilic fraction. The hydrophobic acid components were extracted by suspending the resin in 0.5 M aqueous ammonia solution ($NH_3 \cdot H_2O$) in a glass beaker several times until the supernatant was clear (see Discussion). Both fractions were adjusted to pH 4 with small amounts of

* Address correspondence to either author. (M.L.T.) phone: (515)294-2415; fax: (515)294-3163; e-mail: mlthomps@iastate.edu. (K.S.-R.) phone: (515)294-6105; fax: (515)294-0105; e-mail: srohr@iastate.edu.

[†] Department of Chemistry, Iowa State University.

[‡] Metropolitan Water Reclamation District of Greater Chicago.

[§] Department of Agronomy, Iowa State University.

10.1021/es020821z CCC: $25.00
Published on Web 04/04/2003

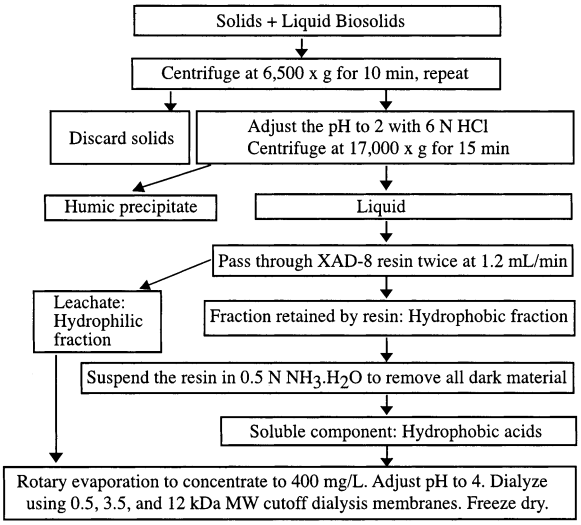

FIGURE 1. Fractionation procedure for biosolids-derived organic matter.

concentrated HCl and then concentrated to 400 mg of C/L using vacuum-rotary evaporation.

BOM components were then separated into MW fractions by using dialysis membranes with MW cutoffs of 0.50, 3.5, and 12.0 kDa. The BOM fractions were dialyzed against distilled, deionized water (1:20) and freeze-dried before subsequent analyses. The elemental composition of the BOM fractions was assessed by high-temperature, dry combustion using a LECO Corp. (St. Joseph, MI) elemental analyzer (C, H, and N) and by inductively coupled plasma mass spectrometry (P and S). Carbon was independently determined by high-temperature combustion of dissolved BOM by using a Shimadzu total organic carbon analyzer.

DRIFT Spectroscopy. DRIFT spectra of a mixture of each BOM fraction and spectroscopic grade KBr (Aldrich Chemical Co.) (~1:250, w/w) were collected by using a Nicolet Magna-IR 560 spectrometer (Nicolet Instrument Corp., Madison, WI). The sample chamber was continuously flushed with CO_2-free dry air. DRIFT spectra were collected from 4000 to 650 cm^{-1} and averaged over 328 scans (resolution $\pm$ 4 cm^{-1}). Functional group analysis of the spectra relied on publications of Williams and Fleming (*19*), Weast (*20*), Stevenson (*21*), Smith (*22*), Naumann (*23*), and Silverstein and Webster (*24*).

NMR Spectroscopy. For all solid-state NMR experiments, samples were packed in 7-mm-diameter zirconia rotors with Kel-F caps and spectra acquired at a ^{13}C frequency of 100 MHz in a Bruker DSX-400 spectrometer. The ^{1}H 90° pulse length was 4.3 μs, and the ^{13}C 180° pulse length for total sideband suppression (TOSS) (*25*) was 6.4 μs. In cross-polarization (CP) experiments, the recycle delay was 1 s. The spinning speeds used were between 5 and 7 kHz. A variety of advanced solid-state NMR techniques were applied: cross-polarization (CP) TOSS, with 40-μs gated decoupling; quantitative direct polarization ^{13}C NMR with 80-s recycle delay (*26*); CH spectral editing (*27*); two-dimensional (2D) HETCOR NMR experiments (*28*) with spin diffusion; separation of undistorted chemical-shift anisotropy (CSA) powder patterns with effortless recoupling (SUPER) (*29*) for determining the CSA of the ^{13}C NMR resonance at around 174.5 ppm; ^{1}H chemical-shift filter experiments with spin diffusion (*30, 31*); and ^{15}N CP/MAS NMR. Solution ^{1}H NMR was also performed. These methods and the parameters used are described in more detail in the Supporting Information.

Results

Elemental Analysis. Before fractionation, the BOM had a low C:N ratio (5.8), consistent with the high degree of microbial decomposition that had transformed wastewater solids to biosolids (Table 1). In general, the hydrophobic fractions of the BOM had greater contents of C and N and smaller contents of P than did the hydrophilic fractions, but a portion of the N content of the hydrophobic fractions reflects ammonium ions added during sample preparation. For both polarity fractions, C:N ratios decreased consistently as MW decreased. The unusually low C content of the 0.5–3.5-kDa hydrophilic fraction reflects an accumulation of Ca, Mg, K, and Na ions that balance the large exchange capacity of that fraction (*2*). The low C:N ratio and relatively high P content specific to the 0.5–3.5-kDa fractions may be due to the accumulation of nucleotides consisting of sugars, N-rich heterocyclic bases, and phosphate. The low C:N ratios are more similar to those of microorganisms than to those of humic substances and are consistent with values reported by Rostad et al. (*32*) for colloids collected from the Mississippi River. These differences in the elemental analyses of the components supported the hypothesis that the hydrophilic/hydrophobic fractionation combined with MW fractionation resulted in chemically distinct groups of compounds.

TABLE 1. Elemental Composition of Biosolids-Derived Organic Matter and Its Components

	(g/100 g)					
sample	C	H	N	P	S	C:N
total BOM	31.3	6.5	5.4	3.2	1.0	5.8
Total Hydrophilic Fractions						
0.5–3.5 kDa	5.1	3.8	4.6	5.4	3.0	1.1
3.5–12 kDa	22.8	5.3	4.8	1.0	1.6	4.7
>12 kDa	23.7	5.6	4.9	1.4	0.2	4.8
Hydrophobic Acid Fractions						
0.5–3.5 kDa	28.7	5.9	8.0	0.5	2.0	3.6
3.5–12 kDa	36.5	6.2	6.5	0.1	2.2	5.6
>12 kDa	37.6	6.3	6.1	0.4	1.5	6.2

Detailed NMR Studies of the High MW Fractions. *One-Dimensional ^{13}C, ^{1}H, and ^{15}N NMR.* The ^{13}C CP/TOSS NMR spectra of >12-kDa hydrophilic and hydrophobic components are given in Figure 2, spectra a and b, respectively. For reference, Figure 2c shows the spectrum of the N-acetylated polysaccharide chitin (poly(*N*-acetyl-1,4-β-D-glucopyranosamine). With some increase in the line broadening, the main features of the spectrum in Figure 2a match those in Figure 2c. Increased line widths as seen here are typical of noncrystalline polymers. They arise from a large number of conformational and packing environments. The spectrum of the high-MW hydrophilic components in Figure 2a (top trace) is particularly simple, exhibiting only five significant bands. They can be assigned to COO/CON groups at 174.5 ppm, anomeric O–CH–O at 100 ppm, OCH around 73 ppm, OCH_3 or NCH between 55 and 65 ppm, and carbon-bonded CH_3 groups at 24–19 ppm. The strong OCH and O–CH–O signals are indicative of a large polysaccharide fraction. The dipolar-dephased spectra (lower traces in Figure 2a,b), which retain signals of unprotonated or mobile groups only, further confirm that the anomeric carbons are protonated and that the peaks near 24 ppm are due to CH_3 groups. It also indicates that the signal near 55 ppm is not due to OCH_3 groups. The ^{13}C CP/MAS/TOSS NMR spectrum of the >12-kDa hydrophobic components (Figure 2b) also shows a large fraction of polysaccharides, but it also reveals some aromatic and substituted aliphatic components with signals near 130 and near 33 and 47 ppm, respectively (Figure 2b, top trace). Since the amount of aromatic and aliphatic compounds is enhanced in the hydrophobic fraction, the polysaccharide content is smaller than that in the hydrophilic fraction. The assignment of the 55 ppm signal to NCH is confirmed by the methine-only spectrum obtained by spectral editing (*27*)

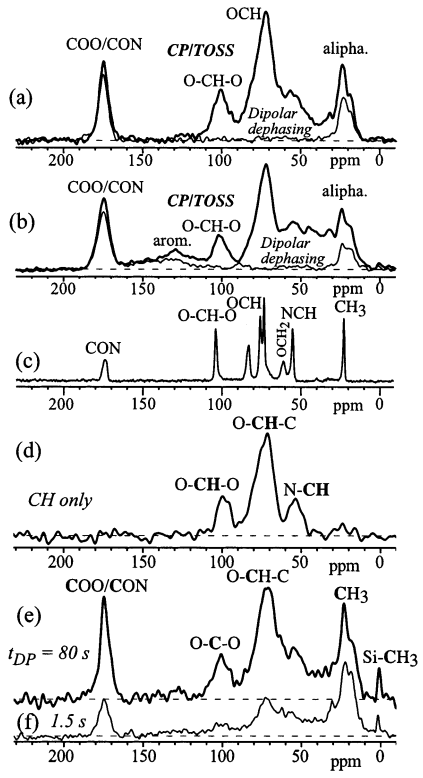

FIGURE 2. 1D ^{13}C NMR spectra of >12-kDa components of the hydrophilic fraction (spectra a and d−f) and the hydrophobic fraction (spectrum b). In both (a) and (b), the top trace is the full CP/TOSS spectrum at 5 kHz and 1-ms CP. The lower trace is CP/TOSS after 40-μs dipolar dephasing, retaining only signal of ^{13}C sites without strong $^{1}H-^{13}C$ dipolar couplings (unprotonated or mobile sites). (c) CP/TOSS spectrum of chitin for reference. (d) Subspectrum showing only CH signals, obtained by spectral editing (*27*). (e) Nearly quantitative DP/TOSS ^{13}C NMR spectrum with a recycle delay of 80 s and a spinning speed of 7 kHz. (f) 7-kHz DP/MAS spectrum with recycle delay of 1.5 s, highlighting the mobile segments in this sample.

(Figure 2d; for details, see below). It also confirms that the signals at 73 and 100 ppm are O−CH−C and O−CH−O groups, respectively, and not $O-CH_2$ or aromatic signals.

For quantitative functional group analysis, Figure 2e shows a nearly quantitative DP/TOSS ^{13}C NMR spectrum of the high-MW hydrophilic component obtained at 7-kHz MAS with a recycle delay of 80 s. It reveals mostly the same signals as the CP spectrum in Figure 2a but exhibits nearly quantitative peak area ratios. The stronger COO/CON signal is particularly noteworthy. In fact, its true intensity is even ca. 15% higher (see Supporting Information). Figure 2f shows a DP ^{13}C NMR spectrum with short recycle delay, which highlights the signal of highly mobile segments with shorter T_{1C} relaxation times.

The ^{1}H solution NMR spectrum of the high-MW hydrophilic fraction (Figure 3a) exhibits a remarkably simple aliphatic region. Only two nonpolar aliphatic proton bands are observed, near 2 and 1.3 ppm. The signal near 2 ppm is assigned to CH_3 groups of acetyl or *N*-acetyl moieties (see below). A similar ^{1}H NMR spectrum was obtained by Repeta et al. (*33*) for DOM in both freshwaters and marine waters (MW > 1 kDa), and the signal near 1.3 ppm was assigned to lipids; however, we will show strong evidence below that this is another CH_3 signal. Figure 3b displays the ^{15}N CP/MAS NMR spectrum of the high-MW hydrophilic fraction. It shows only a single band, which is assigned to (C═O)−(N−H) groups. Specifically, there is no significant signal from $-NH_3^+$ groups, which would resonate near 40 ppm.

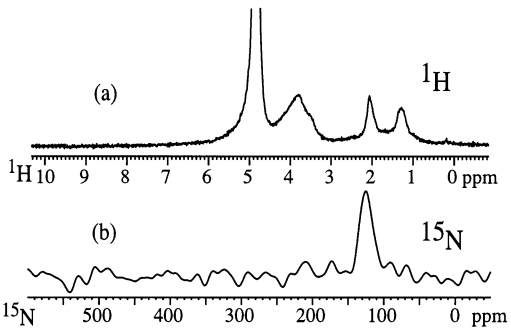

FIGURE 3. (a) 1D ^{1}H solution NMR spectrum. The large peak around 4.9 ppm in spectrum a is that of water (HOD). (b) ^{15}N CP/MAS NMR spectrum of the >12-kDa components of the hydrophilic fraction, recorded at a 7-kHz rotation frequency.

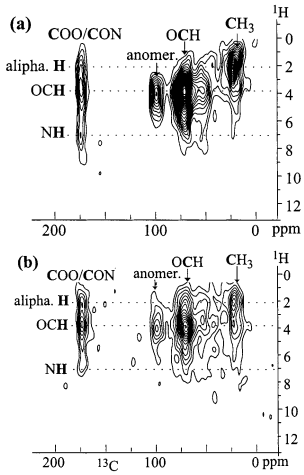

FIGURE 4. 2D HETCOR NMR spectra of >12-kDa components of the hydrophilic fraction. (a) With LGCP of 0.5 ms, showing correlations of protons and carbons separated by three or less bonds. (b) With HH CP of 1 ms, showing correlations of protons and carbons separated by less than 6 Å.

$^{1}H-^{13}C$ HETCOR NMR. Heteronuclear correlation (HETCOR) experiments (*34*), correlating ^{1}H and ^{13}C chemical shifts in 2D spectra, tell us about the protons in the immediate or wider environment of a given carbon (*28*). In particular, we can determine whether COO/CON groups are in close proximity to aromatic, carbohydrate, or aliphatic components. The 2D HETCOR spectra of the hydrophilic fraction shown in Figure 4a,b with two cross-polarization schemes (see Supporting Information) confirm that all sites are in close (<1 nm) proximity (*28*, *34*). For instance, the aliphatic protons are seen to cross-polarize OCH carbons (see Figures S1 and S2 in the Supporting Information). The spectra in Figure 4 reveal that the COO/CON groups are close to OCH and CH_3 protons (e.g., strong 174 ppm ^{13}C peaks are seen at both aliphatic and OCH proton chemical shifts; see Figures S1 and S2). In addition, the COO/CON carbons are also close to protons resonating at ~8 ppm. Since no aromatic rings are observed in the ^{13}C spectra, these protons are identified as N−H protons. Because the high COO/CON isotropic ^{13}C chemical shift as well as its chemical-shift anisotropy exclude COOC ester functionalities (see below), the connection of the carbon-bonded CH_3 groups to the sugar backbone must occur through −CO−NH amide linkages. Such $CH_3-CO-NH$ (*N*-acetyl) groups are common constituents of polysaccharides in bacteria and higher organisms. Usually, the C2 sugar carbon is N-acetylated.

The strong cross-peak of the COO/CON carbon signal with OCH protons near 4 ppm indicates that some COO/CON groups are bonded to *O*-alkyl groups. The absence of

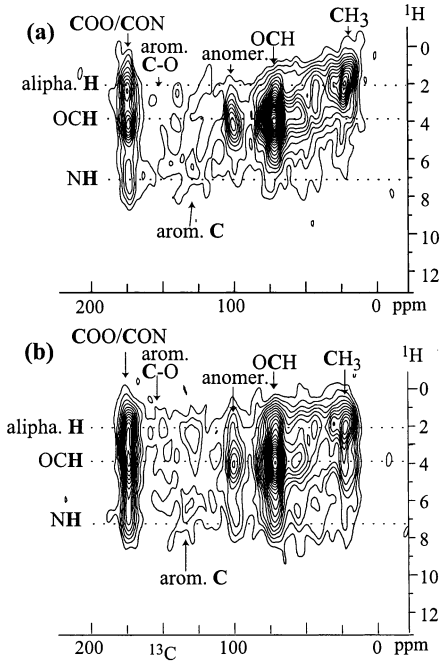

FIGURE 5. 2D HETCOR NMR spectra of >12-kDa components of the hydrophobic fraction. (a) With LGCP of 0.5 ms, showing correlations of protons and carbons separated by three or less bonds. (b) With 1-ms Hartmann−Hahn CP showing correlations of protons and carbons separated by less than 6 Å.

COOH proton signals at >10 ppm indicates that no COOH groups are present. In the HETCOR spectra of the hydrophobic fraction (Figure 5), the COO/CON carbon peak again shows three maxima, corresponding to CH_3, OCH, and NH protons near the COO/CON groups (Figures 5a,b and S3). For the ^{13}C sites resonating near 130 ppm, a ^1H chemical shift of ∼7 ppm rather than 5 ppm is observed in the spectra of Figure 5. This suggests that the groups resonating here are aromatic rather than olefinic CH═CH. The dipolar-dephased spectrum of Figure 2b (lower trace) shows that a significant fraction of these sp^2-hybridized carbons is unprotonated. The HETCOR spectrum of Figure 5b indicates that the aromatic carbons are near aliphatic protons but no cross-peak to sugar OCH protons is detected (see Figure S4 in the Supporting Information). This suggests that the aromatic rings are close to the aliphatic components near 40 ppm but separated from the N-acetylated polysaccharides on a >1-nm length scale (*28*). The exact structure of these aromatic components is not clear at this time. The characteristic signals of lignins (*28*) or tannins are not observed here.

^1H Chemical-Shift Filter and Spin Diffusion. The distance of the two methyl resonances from the OCH protons can be characterized by means of ^1H chemical-shift filtering (*31*), spin diffusion, LGCP, and ^{13}C detection. For reference, spectra without selection are shown in Figure 6a,b, with LGCP contact times of 70 and 500 μs, respectively. In the former, protonated carbons are observed almost exclusively, while the latter shows two-bond proton−carbon transfers as well. Figure 6c demonstrates selection of OCH_n and NCH_n protons and suppression of the methyl signals; the LGCP contact time was 70 μs. Figure 6d−f demonstrate longer-range transfer from the O/NCH_n protons, by 500-μs LGCP as well as spin diffusion of 0.1 and 3 ms in spectra e and f, respectively. Both methyl peaks receive magnetization quickly from the O/NCH_n protons, showing that the CH_3 groups are closely associated with the O/NCH_n moieties. The spectra in Figure 6d,e indicate that the transfer to the upfield methyl signal is faster.

^{13}C Chemical-Shift Anisotropies. The COO/CON peak is a dominant signal in the quantitative ^{13}C NMR spectrum of Figure 2e. For identifying COO/CON groups more specifically, ^{13}C chemical shift anisotropies (CSAs) (*35*) have proven useful. They can be measured for each peak in the ^{13}C MAS spectrum by the SUPER NMR method (*29*). Literature data show that the sign of the CSA parameter δ of esters is consistently opposite to that of amides or carboxylates (*36*). This enables distinction of acetyl (ester) and *N*-acetyl (amide) resonances. The examples of CON, COOC, COO^-, and COOH ^{13}C CSA line shapes in Figure 7 confirm this. Due to $\delta < 0$, the CSA line shape of esters exhibits a strong peak on the right, as shown in Figure 7b,d. In contrast, amides have the main peak to the left of the center of the powder pattern ($\delta > 0$), as seen clearly in the *N*-acetyl groups of chitin and *N*-acetyl valine (Figure 7a,c). Spectra e, f, and h of Figure 7 show typical CSA powder patterns of COOH and COO^- groups. The spectrum of the high-MW hydrophilic BOM component (see Figure 7g) has a (broad) peak to the left of the center, resembling roughly the spectrum of chitin in Figure 7a, maybe with a COO^- pattern as found for glucuronide (Figure 7h) added in. It excludes significant contributions from acetyl groups or other esters.

DRIFT Analysis. The challenges of identifying functional groups in natural organic matter (NOM) by using infrared spectroscopy alone have been discussed by previous workers (e.g., refs *21*, *37*, and *38*). Band overlap due to the complexity of molecular environments made definitive assignments of all bands in the DRIFT spectra of the BOM fractions difficult (Figure 8). However, guided by the NMR results, several of the DRIFT bands of the high-MW fractions can be assigned with some confidence and related to spectra of the lower-MW fractions.

Some DRIFT spectral features of the >12-kDa fractions are readily interpreted. For example, the broad band at 3100−3300 cm^{-1} reflects the N−H stretch of amides and the O−H stretch of hydroxyls, which are largely associated with sugar rings, as shown by NMR. Bands near 2964 and 2936 cm^{-1} (somewhat sharper in the hydrophobic than in the hydrophilic fraction) are attributed to asymmetric CH stretch of CH_3 and CH_2 groups, respectively. The broad band centered at ∼1400 cm^{-1} in the patterns of both >12-kDa fractions is attributed to the C−N stretch of primary amide groups as well as to symmetric stretching of the COO bonds in carboxylate. The broad band that peaks at 1653 cm^{-1} is attributed both to C═O stretching in amide moieties and to asymmetric carboxylate stretching. Amide groups are also indicated by the 1540−1560 cm^{-1} bands (amide II, N−H bending, and C−N stretching) in both samples. Leenheer et al. (*18*) assigned a similar group of IR bands of biocolloidal organic matter from the Seine River to *N*-acetyl amino sugars, consistent with the NMR structure determined here.

Origin of the 1716 cm^{-1} shoulder of both >12-kDa fractions is problematic, for there is no NMR evidence to support significant presence of protonated carboxyl groups, ketones, or aldehydes in the >12-kDa samples. Perhaps a fraction of the carboxyl groups remained protonated during freeze-drying, and the intensity of the C═O band is disproportionate to their actual abundance. We are currently investigating the quantity and pK_a values of carboxyl groups in these materials using titration techniques. The intense, broad band in the region of 1020−1120 cm^{-1} in the >12-kDa hydrophilic spectrum reflect polysaccharides (C−C, C−O−C, and $-CH_2-OH$ stretching). The diminished areas of these bands in the hydrophobic fraction spectra suggest that polysaccharides are less abundant in the hydrophobic fraction than in the hydrophilic fractions, consistent with NMR. Boyd et al. (*11*) observed similar IR bands in various fractions of municipal sludge and attributed them to proteinaceous compounds and carbohydrates.

The DRIFT spectrum of the intermediate (3.5−12 kDa) MW hydrophilic fraction was comparable to that of the high-

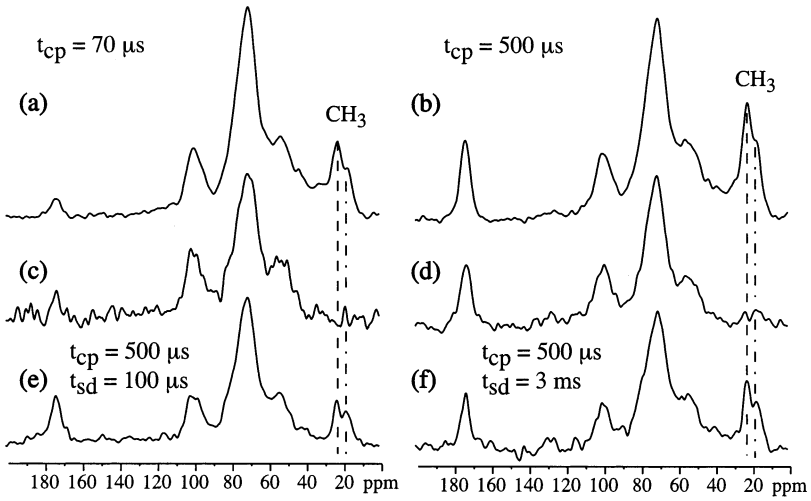

FIGURE 6. ^{1}H chemical shift filter with spin diffusion of >12-kDa components of the hydrophilic fraction. (a) Spectrum without selection shown for reference, with LGCP contact time of 70 μs. (b) Same as spectrum a, with 500-μs LGCP contact time. (c) Spectrum after ^{1}H chemical-shift filter selecting OCH_n and NCH_n protons, which suppresses the methyl signals; LGCP time: 70 μs. (d–f) Spectra after ^{1}H chemical-shift filter selecting OCH_n and NCH_n protons and longer-range transfer from the O/NCH_n protons, by 500-μs LGCP and variable spin diffusion. (d) No spin diffusion. (e) 0.1 ms of spin diffusion (predominantly intramolecular equilibration). (f) 3 ms, which permits detection of protons in a 1-nm distance from the selected O/NCH_n protons.

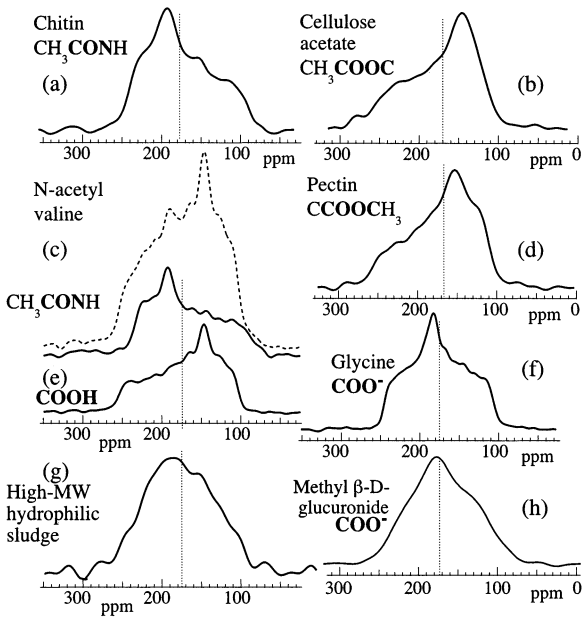

FIGURE 7. Chemical-shift anisotropy powder patterns from 2D SUPER ^{13}C NMR spectra of (a) CONH of chitin; (b) COOC of cellulose acetate; (c) CONH of *N*-acetyl valine and mixed CONH/COOH spectrum (dashed line); (d) COOC of pectin; (e) COOH of *N*-acetyl valine, obtained by difference of the two spectra shown in spectrum c; (f) COO^- of glycine; (g) COO/CONH of >12-kDa components of the hydrophobic fraction; and (h) COO^- of methyl β-D-glucuronide.

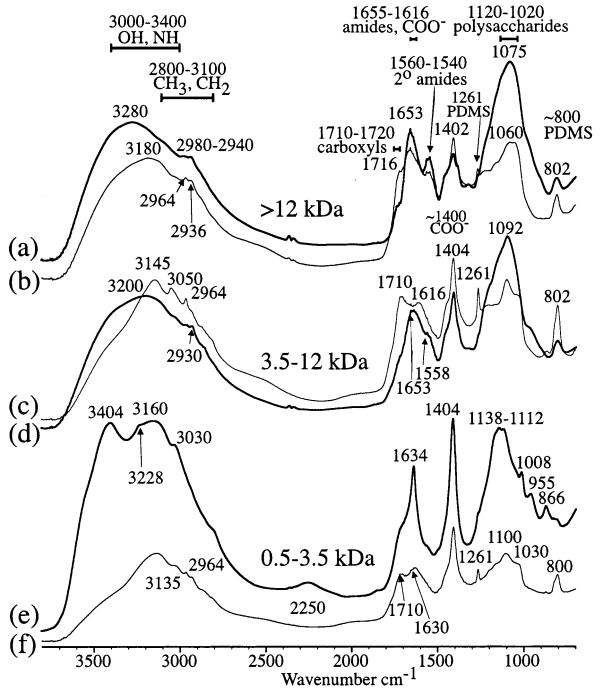

FIGURE 8. DRIFT spectra of BOM fractions. (a, b) >12-kDa components. (c, d) 3.5–12-kDa components. (e, f) 0.5–3.5-kDa components. Bold lines: hydrophilic fractions.

MW fraction (Figure 8). In contrast, the intermediate-MW hydrophobic spectrum differed from its high-MW counterpart with better separation of the 1710 and 1616 cm^{-1} peaks, attributed to C=O stretching of COOH and to asymmetric stretch of C–O in COO^-, respectively. In addition, bands at 3145 and 3050 cm^{-1} of the hydrophobic fraction are attributed to NH stretching of secondary amides and aromatic CH stretching, respectively.

In the DRIFT spectra of the low-MW fractions, again the bands indicative of polysaccharides were more intense in the hydrophilic fraction than in the hydrophobic fraction. There was little evidence of amide groups (1540–1560 cm^{-1}) in the low-MW hydrophilic fraction. The 0.5–3.5-kDa hydrophilic fraction's DRIFT spectrum included additional bands at 1008, 955, and 866 cm^{-1}. Given the higher P content of this fraction, we speculate that these bands might be related to P–O–P functionalities associated with nucleotides. Bands of water molecules are observed at 3404 and 1634 cm^{-1}. Identification of additional bands in the DRIFT spectra is presented in the Supporting Information.

Discussion

Sample Preparation. In retrospect, we realize that use of $NH_3 \cdot H_2O$ to extract hydrophobic components risked unwanted reactions between NH_3(aq) and BOM components. Had such reactions occurred to a significant extent, the DRIFT and NMR spectra of the hydrophilic and hydrophobic BOM

TABLE 2. Comparison of Experimentally Determined Functional Group Composition of >12-kDa Components of Hydrophilic Fraction with Composition of Proposed Structural Model Shown in Figure 9[a]

	CON or COO	OCHO	OCHC	OCH_2	NCH	CCH(C,C)	CH_3	C:N	OCH or NCH	NH	CH_3
model	3	2	7	2	2	0	3	6.3	15	4	9
exp	3.4 ± 0.5	2[b]	7.4 ± 0.5	1.5 ± 1	2 ± 0.3	0.2 ± 0.3	3.2 ± 0.4	5.4	15[b]	6 ± 3	8 ± 4

[a] The experimental data are from quantitative ^{13}C NMR, from $^{1}H-^{13}C$ HETCOR with spin diffusion (proton ratios, last three columns), and from elemental analysis (C:N weight ratio). [b] To facilitate comparison, in the experimental results the OCHO was set to 2, and the OC**H**/NC**H** proton fraction was set to 15; the data of other functional groups were calculated based on their ratios to the amount of OCHO.

components would have been quite dissimilar. The hydrophilic fractions were not treated with $NH_3 \cdot H_2O$, yet DRIFT and NMR spectra reflected similar N-containing moieties as in the hydrophobic fraction. While we do not believe that artifacts were created here, future resin extractions should be done with NaOH.

Identification of *N*-Acetyl Groups. The strong ^{1}H NMR peak near 2 ppm (Figure 3a) and the high 22 ppm ^{13}C NMR peak must be assigned to the methyls of $CH_3-(C{=}O)-$ side groups. By ^{13}C NMR, we can distinguish whether these are acetyl ($CH_3-(C{=}O)-O-$) or *N*-acetyl ($CH_3-(C{=}O)-NH-$) moieties. The isotropic chemical shift of the $^{13}C{=}O$ site is a first indication. Acetyl groups and other esters tend to resonate more upfield than amides and carboxylates (COO^-), quite independent of conformation. For instance, in cellulose acetate (an acetylated polysaccharide), the C=O carbon resonates at 170 ppm, while in chitin (an N-acetylated polysaccharide), the resonance appears at 173.5 ppm. In the high-MW hydrophilic fraction, the resonance is centered at 174.5 ppm with no significant shoulder at 170 ppm. This indicates a predominance of *N*-acetyl (and possibly COO^-) groups in the BOM. The amide bands at 1540 and 1650 cm^{-1} in the DRIFT spectra (Figure 8) can be assigned to the N−H bend in the *N*-acetyl groups.

Further confirmation of this assignment comes from the ^{13}C CSA line shapes in Figure 7. On the basis of the powder patterns of acetylated and N-acetylated compounds, we can interpret the spectrum of the COO/CON groups in the high-MW hydrophilic fraction, shown in Figure 7g. It does not exhibit the peak on the right characteristic of acetate groups (Figure 7b) but rather matches the overall intensity distribution of the *N*-acetyl groups in chitin and *N*-acetyl valine, possibly mixed with COO^- functionalities. COOH groups are excluded by the HETCOR spectra of Figure 4, which exhibit no COOH proton signals near 12 ppm. Thus, most carboxylic acid functionalities that may be present must have given up their protons to become COO^- groups, consistent with the diminished DRIFT bands near 1710 cm^{-1} in the spectra of the hydrophilic fraction. In the HETCOR spectra of Figure 4, the N−H proton signals and their proximity to the sugar rings are seen clearly. The CH_3 signals also quickly develop cross-peaks to NH and OCH resonances, confirming the $CH_3-(C{=}O)-NH-CH-O$ structural unit of the *N*-acetyl group. In summary, many *N*-acetyl but few, if any, acetyl groups are found in this BOM sample.

Identification of N-Acetylated Polysaccharides. The nearly quantitative and the CH-only ^{13}C NMR spectra of the high-MW hydrophilic fraction (Figure 2d,e) give valuable information on its composition. The structure is dominated by O−CH groups, identified as such by their chemical shift and in the methine-only spectrum of Figure 2d, which excludes $O-CH_2-CH_2-O$ groups. They are most likely part of sugar rings, since there is one O−CH−O group per 3.5 other O−CH carbons. Most likely, they form polysaccharide chains given the high molecular weight of this fraction. There is approximately one NCH group per O−CH−O site, per *N*-acetyl CH_3 (downfield methyl peak in Figure 2e,f), per 3.5 O−CH, and per 1.7 COO/CON carbons. In addition, there is evidence of an $O-CH_2$ resonance that fills the "valley" between the O−CH and the N−CH peaks in the ^{13}C spectrum of Figure 2e. The DRIFT spectra of Figure 8a confirm the NMR analysis, with bands at 3300 and 1080 cm^{-1} assigned to OH and C−O stretch, respectively, of polysaccharides and bands at 1650 and 1540 cm^{-1} assigned to the OCNH amide groups (*39*).

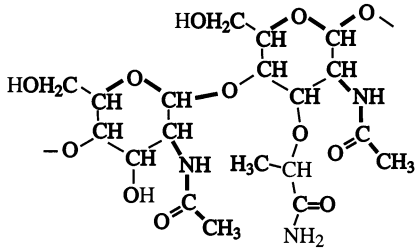

FIGURE 9. Structural model for the high-MW hydrophilic component. It corresponds to a peptidoglycan found in bacterial cell walls after removal of the oligopeptide chains. Structural units that have been identified specifically by NMR are highlighted in bold. For comparison with the experimental data, see Table 2.

Structural Model with a Second Side Group. The data discussed so far clearly show the presence of a large fraction of *N*-acetyl groups bonded to a polysaccharide backbone. Nevertheless, the quantitative analysis and the comparison with the spectrum of chitin (see Figure 2c) indicate that there are additional CH_3 and CO groups in the structure. For instance, the ^{13}C NMR spectra of Figure 2f or Figure 6e exhibit a second methyl signal near 20 ppm, upfield from the *N*-acetyl CH_3 resonance. The strength of the NH proton signals in the HETCOR spectra and the low C:N ratio also indicate the presence of additional NH_n groups. In contrast, no additional NCH groups can be accounted for in the spectra of Figure 2, which excludes significant peptide fractions. The ^{1}H spin diffusion experiments after ^{1}H chemical shift filtering displayed in Figure 6 prove that both types of methyl groups are closely associated with the polysaccharides. The second CH_3 group should have a different ^{1}H chemical shift, upfield from the *N*-acetyl CH_3 signal. Indeed, the ^{1}H spectrum of Figure 3a shows a second distinct aliphatic peak that can be assigned to CH_3 protons. In addition, the HETCOR spectrum of Figure 4 indicates that the 20 ppm ^{13}C peak is associated with a more upfield ^{1}H chemical shift. On this basis, we assign the 1.3 ppm peak in the ^{1}H spectrum to CH_3 groups and not to lipids as suggested in ref *33*. In the ^{1}H spectrum of Figure 3a, the area ratio of ca. 3:1 of the OCH/NCH signals near 4 ppm relative to the 2 ppm CH_3 signal confirms that the 2 ppm peak represents only one CH_3 group.

All requirements described here are fulfilled quite well by the structural model shown in Figure 9. Basically, it is an N-acetylated polysaccharide, but every other repeat unit bears a second side group. Its structure, $O-CH(CH_3)-(C{=}O)-NH_2$, accounts for the CH_3 signal upfield of the *N*-acetyl CH_3 signal in both ^{13}C and ^{1}H spectra; the additional C=O intensity was detected in the quantitative ^{13}C spectrum; the NH_2 group decreases the C:N ratio and increases the amide−proton fraction, consistent with their strong intensity in the HETCOR spectra of Figure 4; and the OCH group can be accounted

for in the OCH ^{13}C and ^{1}H NMR signals. The $CONH_2$ and CONH signals would both contribute to the same broad band in the ^{15}N spectrum. No additional NCH groups nor specific CCH/CCH_2 groups not bonded to O or N are introduced, in agreement with the ^{13}C and ^{1}H NMR spectra. The structure proposed in Figure 9 closely resembles that of peptidoglycans in bacterial cell walls (*40*), which consist of glucosamine (left monomer unit shown) and muramic acid connected to oligopeptides by a peptide bond. According to the NMR spectra, in the high-MW hydrophilic BOM fraction, most of the oligopeptides have been clipped off. The C:N ratio suggests that occasional alanine residues (C:N = 3:1) may still be attached to the longer side group. However, the amount of such peptides must be quite small; otherwise, the NCH:OCHO ratio would exceed the 1:1 ratio determined by NMR. Table 2 shows good agreement between the composition determined by experiment and that of the model structure shown in Figure 9. While the structure contains no COO^- groups, it should be noted that the NMR data do not exclude some carboxylates, as in uronic acids.

Comparison with Other DOM. The high-MW hydrophilic component shows significant similarities with a >1.0-kDa DOM fraction from freshwaters and marine waters (*33*, *41*). Aluwihare et al. (*41*) identified this component as decomposition residues of algal exudates (*41*), characterizing it oligosaccharides with 40% acetylation. This resembles the structures that we have found, except that we have shown the polysaccharides to be N-acetylated. Note that the structural model proposed by Repeta et al. (*33*) does not explain the 15:1 C:N ratio of their samples. In agreement with our structural results, Leenheer et al. also have interpreted IR spectra of natural DOM in terms of *N*-acetyl amino sugar (*18*).

The lower-MW fractions (i.e., 0.50−3.5 and 3.5−12.0 kDa) were similar to their high-MW counterparts in some respects. For example, polysaccharide IR absorptions dominated the hydrophilic spectra. In contrast, the abundance of carboxyl groups, suggested by the intensity of absorption in the 1400 and 1720 cm^{-1} regions, increased with decreasing MW in the hydrophilic fractions but was greatest in the 3.5−12.0 kDa fraction of the hydrophobic components. Proton binding will be measured to quantitatively corroborate this interpretation.

Acknowledgments

We thank A. Carmo, L. Schultz, L. Weldon, and P. Schultz for technical assistance and fruitful discussions. We gratefully acknowledge funding from the U.S. Department of Agriculture NRI Grant 98-35102-6756. This is Journal Paper No. J-19298 of the Iowa Agriculture & Home Economics Experiment Station, Ames, IA. Project No. 3359, supported by Hatch Act and State of Iowa funds.

Supporting Information Available

More detailed descriptions of the BOM extraction method, NMR methods, cross-sections through the HETCOR NMR spectra, discussion of additional DRIFT bands, and a table with DRIFT peak assignments. This material is available free of charge via the Internet at http://pubs.acs.org.

Literature Cited

(1) Nor, Y. M.; Cheng, H. H. *Environ. Toxicol. Chem*. **1986**, *5*, 941.
(2) Han, N.; Thompson, M. L. *J. Environ. Qual.* **1999**, *28*, 939.
(3) Keefer, R. F.; Codling, E. E.; Singh, R. N. *Soil Sci. Soc. Am. J.* **1984**, *48*, 1054.
(4) Qualls, R.; Haines, B. L. *Soil Sci. Soc. Am. J.* **1991**, *55*, 1112.
(5) Nelson, S. D.; Letey, J.; Farmer, W. J.; Williams, C. F.; Ben-Hur, M. *J. Environ. Qual.* **1998**, *27*, 1194.
(6) Novak, J. M.; Bertch, P. M.; Mills, G. L. *J. Environ. Qual.* **1992**, *21*, 537.
(7) Averett, R. C. *Humic Substances in the Suwannee River, Georgia*: *Interactions, Properties, and Proposed Structures*; U.S. Geological Survey: Denver, CO, 1994.
(8) Boyd, S. A.; Sommers, L. E.; Nelson, D. W. *Soil Sci. Soc. Am. J.* **1980**, *44*, 1179.
(9) Sposito, G.; Holtzclaw, K. M.; LeVesque, C. S.; Johnston, C. T. *Soil Sci. Soc. Am. J.* **1982**, *46*, 265.
(10) Sposito, G.; Holtzclaw, K. M.; Baham, J. *Soil Sci. Soc. Am. J.* **1976**, *40*, 691.
(11) Boyd, S. A.; Sommers, L. E.; Nelson, D. W. *Soil Sci. Soc. Am. J.* **1979**, *43*, 893.
(12) Zhou, L. X.; Yang, H.; Shen, Q. R.; Wong, M. H.; Wong, J. W. C. *Environ. Technol.* **2000**, *21*, 765.
(13) Sposito, G.; Schaumberg, G. D.; Perkins, T. G.; Holtzclaw, K. M. *Environ. Sci. Technol.* **1978**, *12*, 931.
(14) Leenheer, J. A. *Environ. Sci. Technol.* **1981**, *15*, 578.
(15) Swift, R. S. In *Humic Substances in Soil, Sediment, and Water*; Aiken, G. R., McKnight, D. M., Wershaw, R. L., Eds.; John Wiley & Sons: New York, 1989; p 387.
(16) Muller, M. B.; Schmitt, D.; Frimmel, F. *Environ. Sci. Technol.* **2000**, *34*, 4867.
(17) Hundal, L. S.; Carmo, A. M.; Bleam, W. F.; Thompson, M. L. *Environ. Sci. Technol.* **2000**, *34*, 5184.
(18) Leenheer, J. A.; Croue, J. P.; Benjamin, M.; Korshin, G. V.; Hwang, C. J.; Bruchet, A.; Aiken, G. R. In *Natural Organic Matter and Disinfection By-Products*; Barrett, S., Krasner, S. W., Amy, G. L., Eds.; ACS Symposium Series 761; American Chemical Society: Washington, DC, 2000; p 68.
(19) Williams, D. H.; Fleming, L. *Spectroscopic Methods in Organic Chemistry*; McGraw-Hill: New York, 1973.
(20) Weast, R. C. *CRC Handbook of Chemistry and Physics*; CRC Press: Boca Raton, FL, 1980.
(21) Stevenson, F. J. *Humus Chemistry*: *Genesis, Composition, Reactions*, 2nd ed.; John Wiley & Sons: New York, 1994.
(22) Smith, B. *Infrared Spectral Interpretation*: *A Systematic Approach*; CRC Press: Boca Raton, FL, 1999.
(23) Naumann, D. In *Encyclopedia of Analytical Chemistry*; Meyers, R. A., Eds.; John Wiley & Sons: New York, 2000; p 102.
(24) Silverstein, R. M.; Webster, F. X. *Spectrometric Identification of Organic Compounds*, 6th ed.; John Wiley: New York, 1998.
(25) Mao, J.-D.; Schmidt-Rohr, K. *Abstracts of 43rd Experimental Nuclear Magnetic Resonance Conference*; 2002; p 214.
(26) Mao, J.-D.; Hu, W.-G.; Schmidt-Rohr, K.; Davies, G.; Ghabbour, E. A.; Xing, B. *Soil Sci. Soc. Am. J.* **2000**, *64*, 873.
(27) Schmidt-Rohr, K.; Mao, J.-D. *J. Am. Chem. Soc.* **2002**, *124*, 13938−13948.
(28) Mao, J.-D.; Xing, B.; Schmidt-Rohr, K. *Environ. Sci. Technol.* **2001**, *35*, 1928.
(29) Liu, S.-F.; Mao, J.-D.; Schmidt-Rohr, K. *J. Magn. Reson.* **2002**, *155*, 15.
(30) Schmidt-Rohr, K.; Clauss, J.; Blumich, B.; Spiess, H. W. *Magn. Reson. Chem.* **1990**, *28*, s3.
(31) Clauss, J.; Schmidt-Rohr, K.; Spiess, H. W. *Acta Polym.* **1993**, *44*, 1.
(32) Rostad, C. E.; Leenheer, J. A.; Daniel, S. R. *Environ. Sci. Technol.* **1997**, *31*, 3218.
(33) Repeta, D. J.; Quan, T. M.; Aluwihare, L. I.; Accardi, A. *Geochim. Cosmochim. Acta* **2002**, *66*, 955.
(34) Caravatti, P.; Bodenhausen, G.; Ernst, R. R. *Chem. Phys. Lett.* **1982**, *89*, 363.
(35) Schmidt-Rohr, K.; Spiess, H. W. *Multidimensional Solid-State NMR and Polymers*; Academic Press: San Diego, CA, 1994.
(36) Duncan, T. M. *A Compilation of Chemical Shift Anisotropy*; Farragut: Chicago, 1990.
(37) MacCarthy, P.; Rice, J. A. In *Humic Substances in Soil, Sediment, and Water*; Aiken, G. R., McKnight, D. M., Wershaw, R. L., Eds.; John Wiley & Sons: New York, 1985; p 527.
(38) Baes, A. U.; Bloom, P. R. *Soil Sci. Soc. Am. J.* **1989**, *53*, 695.
(39) Yoshimizu, H.; Asakura, T. *J. Appl. Polym. Sci.* **1990**, *40*, 1745.
(40) Lehninger, A. L.; Nelson, D. C.; Cox, M. M. *Principles of Biochemistry*; Worth Publishers: New York, 1993.
(41) Aluwihare, L. I.; Repeta, D. J.; Chen, R. F. *Nature* **1997**, *387*, 166.

Received for review July 5, 2002. Revised manuscript received February 11, 2003. Accepted February 12, 2003.

ES020821Z